D. Bhanu Prakash, D. K. K. Vamsi*, D. Bangaru Rajesh, and Carani B Sanjeevi

Control Intervention Strategies for Within-Host, Between-Host and their Efficacy in the Treatment, Spread of COVID-19 : A Multi Scale Modeling Approach

Abstract: The COVID-19 pandemic has resulted in more than 65.5 million infections and 15,14,695 deaths in 212 countries over the last few months. Different drug intervention acting at multiple stages of pathogenesis of COVID-19 can substantially reduce the infection induced,thereby decreasing the mortality. Also population level control strategies can reduce the spread of the COVID-19 substantially. Motivated by these observations, in this work we propose and study a multi scale model linking both within-host and between-host dynamics of COVID-19. Initially the natural history dealing with the disease dynamics is studied. Later comparative effectiveness is performed to understand the efficacy of both the within-host and population level interventions. Findings of this study suggest that a combined strategy involving treatment with drugs such as Arbidol, remdesivir, Lopinavir/Ritonavir that inhibits viral replication and immunotherapies like monoclonal antibodies, along with environmental hygiene and generalized social distancing proved to be the best and optimal in reducing the basic reproduction number and environmental spread of the virus at the population level.

Keywords: COVID-19 ; Multi scale modeling; Within-host; Between-host; Comparative Effectiveness

MSC: 37Nxx; 92BXX; 92Cxx

1 introduction

The pandemic COVID-19, caused by SARS-CoV-2, spread its tentacles through out the world by taking lives of 15,14,695 people and livelihood of many more across the globe. Research communities across the world are racing against time in contributing their piece of knowledge in tackling this virus [1].

Mathematical models play a crucial role in this journey as they are helpful in multi-fold. Firstly, they help in Understanding the dynamics of infection and its spread in the society. They help in studying the success of various control measures that can be implemented in order to avoid further damage. Secondly, the within-host mathematical modeling helps to study the dynamics of virus in the human body and can help us in understanding efficacy of different drug intervention acting at multiple stages of pathogenesis which in turn can help in identification of potential vaccine candidates. Some of the works dealing with population level studies and within-host studies for diseases such as Dengue, HIV, Influenza include [6, 16, 5] and references within. Recent works dealing with population level studies and within-host studies for COVID-19 can be found

D. Bhanu Prakash, D. Bangaru Rajesh: Department of Mathematics and Computer Science, Sri Sathya Sai Institute of Higher Learning - SSSIHL, India, E-mail: bhanuprakash@sssihl.edu.in, bangaru.dmacs@gmail.com
*Corresponding Author: D. K. K. Vamsi: Department of Mathematics and Computer Science, Sri Sathya Sai Institute of Higher Learning - SSSIHL, India, E-mail: dkkvamsi@sssihl.edu.in
Carani B Sanjeevi: Vice-Chancellor, Sri Sathya Sai Institute of Higher Learning - SSSIHL, India
and Department of Medicine, Karolinska Institute, Stockholm, Sweden, E-mail: sanjeevi.carani@sssihl.edu.in, sanjeevi.carani@ki.se

in [7, 8, 9, 10, 15]. The transmission dynamics for various viruses like Nipha virus and Ebola virus are studied using mathematical models to study the efficiency of various control interventions[2, 12].

In addition to these, there are multi scale models linking within-host and between-host population scales which helps us understand not only the efficacy of the intervention at individual level but also the effectiveness at the population level. Broadly there are five different categories of multi scale models. As enlisted in [6], they are Individual-based multi scale model, nested multi scale model, embedded multi scale model, hybrid multi scale model and coupled multi scale model. Few works involving multi scale modeling approaches for diseases include [6, 17]. To the best of our knowledge, there is no work dealing with multi scale modeling approach for COVID-19.

Motivated by the above in this study, we propose and study a nested multi scale model. Using the technique of comparative effectiveness. We study the effectiveness of drug interventions and population level control measures at varied efficacy levels. The multi scale model and the corresponding interventions study which is being attempted here is the first of its kind for COVID-19.

2 The Multi Scale Model Formulation

The multi scale model for COVID-19 disease dynamics across two scales that are within-host and between-host. The model consists of eight compartments involving susceptible epithelial cells S_h, infected epithelial cells I_h, SARS-CoV-2 viral load V_h at within-host scale and susceptible human population S_p, exposed population E_p, infected population I_p, recovered populations R_p and environmental viral load V_p at between-host scale. The assumptions for the proposed model include the following.

1. The within-host dynamics are assumed to occur at fast time scale s while the dynamics of the between-host scale variables is assumed to occur at slow time scale t.

2. We assume that SARS-CoV-2 virus can be transmitted only through environmental(indirect) transmission.

3. We do not consider the asymptomatic patients for this study as there is no sufficient evidence of within-host dynamics of asymptomatic patients. We employ the basic SEIR model at between-host level.

Based on the above assumptions we propose the following multi scale model for COVID-19.

$$\frac{\mathrm{d}S_h(s)}{\mathrm{d}s} = -\beta S_h(s)V_h(s)$$

$$\frac{\mathrm{d}I_h(s)}{\mathrm{d}s} = \beta S_h(s)V_h(s) - (d_1 + d_2 + d_3 + d_4 + d_5 + d_6)I_h(s) - \mu I_h(s)$$

$$\frac{\mathrm{d}V_h(s)}{\mathrm{d}s} = \alpha I_h(s) - (b_1 + b_2 + b_3 + b_4 + b_5 + b_6)V_h(s) - \alpha_h V_h(s)$$

$$\frac{\mathrm{d}S_p(t)}{\mathrm{d}t} = \pi_p - \mu_p S_p(t) - \frac{\eta_p S_p(t)I_p(t)}{N_p(t)} - \eta_w S_p(t)V_p(t)$$

$$\frac{\mathrm{d}E_p(t)}{\mathrm{d}t} = \frac{\eta_p S_p(t)I_p(t)}{N_p(t)} + \eta_w S_p(t)V_p(t) - (\omega_p + \mu_p)E_p(t)$$

$$\frac{\mathrm{d}I_p(t)}{\mathrm{d}t} = \omega_p E_p(t) - (\tau_p + \mu_p)I_p(t)$$

$$\frac{\mathrm{d}R_p(t)}{\mathrm{d}t} = \tau_p I_p(t) - \mu_p R_p(t)$$

$$\frac{\mathrm{d}V_p(t)}{\mathrm{d}t} = V_h(s)\alpha_h I_p(t) - \pi V_p(t) \tag{2.1}$$

The first compartment in the model 2.1 deals with the dynamics of susceptible epithelial cells $S_h(s)$. They decrease at a rate β following contact with the virus. The second compartment deals with the dynamics of infected epithelial cells. They are increased through infection of susceptible cells and are decreased through clearance by cytokines and chemokines such as IL-6, TNF-α, CCL5, CXCL8, CXCL10 at the rate $d_1, d_2, d_3, d_4,$ d_5 and d_6 respectively and through natural death at a rate μ. Compartment three deals with SARS-CoV-2 viral

load. The viral load is increased due to reproduction of virus in the infected cells at the rate α. This viral load is decreased due to clearance by cytokines and chemokines such as IL-6, TNF-α, CCL5, CXCL8, CXCL10 at the rate b_1, b_2, b_3, b_4, b_5 and b_6 respectively and they are released into environment at a rate α_h. The term α_h links within-host and between-host scales in a uni-directional way.

We assume that the total human population N_p in the between-host dynamics is divided into four sub-groups denoted by S_p, E_p, I_p and R_p which represent respectively, the susceptible, exposed, infected and recovered or the removed population. Compartment 4 in the model (2.1) describes the dynamics of suscep-tible humans. They are assumed to be supplied at a constant rate π_p through birth and are removed at the natural death rate μ_p. They are also reduced by interaction with infected cells and virus in the environment through the terms $\frac{\eta_p S_p(t) I_p(t)}{N_p(t)}$ and $\eta_w S_p(t) V_p(t)$ respectively. Compartment 5 describes the dynamics of exposed humans. They become exposed due to contacts with either infected people or virus particles through the terms $\frac{\eta_p S_p(t) I_p(t)}{N_p(t)}$ and $\eta_w S_p(t) V_p(t)$ respectively. They are removed at the natural death rate μ_p and the rate at which they become infected through ω_p. Compartment 6 describes the dynamics of infected humans. Exposed hu-mans become infected after the incubation period at the rate ω_p. They are reduced through medication or natural death at the rate τ_p and μ_p respectively. Compartment 7 describes the dynamics of recovered individ-uals. Infected humans are recovered at the rate τ_p and are removed due to natural death at the rate μ_p. Finally compartment 8 describes the dynamics of viral load in the environment.The viral load in the environment is contributed by infected cells at the rate $\alpha_h V_h$ through coughing/sneezing. The virus particles cannot live in environment without invading into host cell for long time. The virus will get killed at the rate π. The values for a few within-host parameters are not available with respect to COVID-19. Since COVID-19 is similar to IAV as can be seen from [13], we chose these parameter values from IAV models [6]. The values for these various parameters is given in table 1.

Table 1: Table describing the parameter values

Variable	Description	Value	Units	Source
π_p	Birth rate	248.62	d^{-1}	[11]
μ_p	Natural mortality rate	0.062	d^{-1}	[11]
η_p	Contact rate	0.274	d^{-1}	[11]
η_w	Disease transmission coefficient	0.000001231	d^{-1}	[8]
ω_p	Incubation Period	0.1961	d^{-1}	[3]
τ_p	Removal or recovery of I_p	0.14	d^{-1}	[3]
π	Removal rate of virus from environment	2.88	d^{-1}	[6]
β	Rate at which healthy Pneumocytes are infected	0.55	$d^{-1} score^{-1}$	[10]
μ	Natural death rate of Type II Pneumocytes	0.11	d^{-1}	[10]
α	Burst rate of virus particles	0.24	d^{-1}	[10]
α_h	shedding rate of virus from infected human	5.36	d^{-1}	[10]
d_1,d_2,d_3,d_4,d_5,d_6	Rate at which infected Pneumocytes are removed because of the release of cytokines IL-6,TNF-α,CCL 5, CXCL 8,CXCL-10,INF-α respectively	0.01533	$cell^{-1} d^{-1}$	[6]
b_1,b_2,b_3,b_4,b_5,b_6	Rate at which viral particles are removed because of the release of cytokines IL-6,TNF-α,CCL 5, CXCL 8,CXCL-10,INF-α respectively	250	$cell^{-1} d^{-1}$	[6]

The initial values for the different between-host human population are listed in the table 2.

Table 2: Table describing the initial values for between-host compartments

Variable	Description	Initial Values	Source
$S_h(s)$	Susceptible target cells	3.2×10^5	[16]
$I_h(s)$	Infected target cells	0	Assumed
$V_h(s)$	Viral load within infected cells	3.0	[16]
$S_p(t)$	Susceptible Individuals	4000	[11]
$E_p(t)$	Exposed Individuals	0	Assumed
$I_p(t)$	Infected Individuals	10	[11]
$R_p(t)$	Recovered Individuals	0	Assumed
$V_p(t)$	Community Viral load	100	Assumed

3 The reduced-order multi scale model

There are two difficulties in working with the proposed multi scale model.

1. Time scale mismatch: The within-host scale is in terms of a fast time scale s, while the between-host scale is in terms of a slow time scale t.

2. Transient $V_h(s)$: $V_h(s)$ remains non-zero only for a short period since the infection remains only for few days.

These problems can be overcome by changing the measure of host-infectiousness from $V_h(s)$ to a new quantity N_h (the area under the viral load curve). If we denote s_{d_1} and s_{d_2} as the times at which viral load takes the value of detection limit at the beginning and at the end of the infection, then $s_{d_2} - s_{d_1}$ can be taken as the duration of host infectiousness. Then the amount of virus produced N_h is given as :

$$N_h = \int_{s_{d_1}}^{s_{d_2}} V_h \, ds$$

We follow the approach given in [6] to derive the expression for N_h.

We get the reduced multi scale model as

$$\frac{dS_p(t)}{dt} = \pi_p - \mu_p S_p(t) - \frac{\eta_p S_p(t) I_p(t)}{N_p(t)} - \eta_w S_p(t) V_p(t)$$

$$\frac{dE_p(t)}{dt} = \frac{\eta_p S_p(t) I_p(t)}{N_p(t)} + \eta_w S_p(t) V_p(t) - (\omega_p + \mu_p) E_p(t)$$

$$\frac{dI_p(t)}{dt} = \omega_p E_p(t) - (\tau_p + \mu_p) I_p(t)$$

$$\frac{dR_p(t)}{dt} = \tau_p I_p(t) - \mu_p R_p(t)$$

$$\frac{dV_p(t)}{dt} = N_h \alpha_h I_p(t) - \pi V_p(t) \tag{3.1}$$

where

$$N_h = \frac{\mathfrak{R}_\circ}{\beta} \left[1 - e^{-\mathfrak{R}_\circ} - \mathfrak{R}_\circ e^{-2\mathfrak{R}_\circ} \right]$$

with the initial conditions $S_p(0) \geq 0$, $E_p(0) \geq 0$, $I_p(0) \geq 0$, $R_p(0) \geq 0$ and $V_p(0) \geq 0$.

The basic reproductive number for the within-host scale sub model in model 2.1 is given by

$$\mathfrak{R}_\circ = \frac{\alpha \beta S_0}{(b_1 + b_2 + b_3 + b_4 + b_5 + b_6 + \alpha_h)(d_1 + d_2 + d_3 + d_4 + d_5 + d_6 + \mu)} \tag{3.2}$$

Adding the compartments for the sub model 3.1, we get the dynamics of total population governed by the following equation.

$$\frac{\mathrm{d}N_p(t)}{\mathrm{d}t} = \pi_p - \mu_p N_p(t)$$

The feasible region for the model (3.1) is given by

$$\Omega = \left\{ (S_p(t), E_p(t), I_p(t), R_p(t)) \in \mathbb{R}_+^4 : N_p(t) \le \frac{\pi_p}{\mu_p}, \ V_p(t) \in \mathbb{R}_+ : V_p(t) \le \frac{N_h \alpha_h}{\pi} \frac{\pi_p}{\mu_p} \right\}$$

4 Stability Analysis of the reduced multi scale model

In this section, we do the stability analysis for the reduced multi scale model 3.1.

4.1 Disease free equilibrium and R_0

The disease-free equilibrium for the model 3.1 is given by

$$E^0 = \left(S_p^0, E_p^0, I_p^0, R_p^0, V_p^0 \right) = \left(\frac{\pi_p}{\mu_p}, 0, 0, 0, 0 \right)$$

We now calculate the basic reproduction number of the multi scale model 3.1 using the next generation matrix approach [14].

The Jacobian evaluated at the disease-free equilibrium, E^0, is given by

$$J(E^0) = \begin{bmatrix} -(\omega_p + \mu_p) & \eta_p & \frac{\eta_w \pi_p}{\mu_p} \\ \omega_p & -(\tau_p + \mu_p) & 0 \\ 0 & N_h \alpha_h & -\pi \end{bmatrix}$$

The $J(E^0)$ can be decomposed into two matrices F and V such that $J(E^0) = F - V$, where F is the transmission and non-negative matrix describing the generation of secondary infections and V is the transition and non-singular matrix, describing the changes in individual states such as removal by death, recovery and excretion of SARS-CoV-2 into the environment by infected human in the community. Since the environment acts as a reservoir of the infective pathogen, we have,

$$F = \begin{bmatrix} 0 & \eta_p & \frac{\eta_w \pi_p}{\mu_p} \\ 0 & 0 & 0 \\ 0 & N_h \alpha_h & 0 \end{bmatrix}, V = \begin{bmatrix} (\omega_p + \mu_p) & 0 & 0 \\ -\omega_p & (\tau_p + \mu_p) & 0 \\ 0 & 0 & \pi \end{bmatrix}$$

The basic reproductive number is given by the spectral radius (dominant eigenvalue) of the matrix FV^{-1}. So in this case, we have the basic reproduction number of the system 3.1 to be

$$\mathcal{R}_0 = \frac{\eta_p \omega_p + \sqrt{(\eta_p \omega_p)^2 + \frac{4\eta_w \pi_p N_h \alpha_h \omega_p (\omega_p + \mu_p)(\tau_p + \mu_p)}{\mu_p \pi}}}{2(\omega_p + \mu_p)(\tau_p + \mu_p)} \tag{4.1}$$

Theorem 1: The DFE E^0 of the system 3.1 is locally asymptotically stable if $\mathcal{R}_0 < 1$.

Proof: The Jacobian matrix evaluated at E^0 is given by

$$J(E^0) = \begin{bmatrix} -\mu_p & 0 & -\eta_p & 0 & -\frac{\eta_w \pi_p}{\mu_p} \\ 0 & -(\omega_p + \mu_p) & \eta_p & 0 & \frac{\eta_w \pi_p}{\mu_p} \\ 0 & \omega_p & -(\tau_p + \mu_p) & 0 & 0 \\ 0 & 0 & \tau_p & -\mu_p & 0 \\ 0 & 0 & N_h \alpha_h & 0 & -\pi \end{bmatrix}$$

From the above jacobian matrix, it can be seen that the two of the eigen values are given by $-\mu_p$ (repeated twice). The rest can be obtained through the characteristic equation given below.

$$\lambda^3 + a_1\lambda^2 + a_2\lambda + a_3 = 0,$$

where

$$a_1 = \pi + \omega_p + \tau_p + 2\mu_p$$
$$a_2 = (\omega_p + \mu_p)(\tau_p + \mu_p) + \pi(\omega_p + \tau_p + 2\mu_p) - \omega_p\eta_p$$
$$a_3 = (\omega_p + \mu_p)(\tau_p + \mu_p)\pi - \omega_p(\pi\eta_p + \frac{\eta_w\pi_p N_h\alpha_h}{\mu_p})$$

When $\mathcal{R}_0 < 1$, a_2, a_3 are positive. Since a_1 has all positive terms, all the coefficients of the characteristic equation are positive when $\mathcal{R}_0 < 1$. Further, by Routh-Hurtwiz criterion for a third order polynomial, we get that all the eigen values of the characteristic polynomial to be negative as $a_i's > 0$, for $i = 1, 2, 3$.[4]. Hence the DFE E^0 is locally asymptotically stable when $\mathcal{R}_0 < 1$ as all the eigen values of the jacobian matrix are negative.

4.2 Endemic equilibrium

Let $\overline{E} = (\overline{S_p}, \overline{E_p}, \overline{I_p}, \overline{R_p}, \overline{V_p})$ denote the endemic equilibrium point of the system 3.1. To get the endemic equilibrium, we set the left-hand side of the equations of the model system 3.1 equal to zero and determine the nontrivial solution of the resulting algebraic equations, which gives

$$\overline{S_p} = \frac{1}{\mu_p}[\pi_p - \frac{(\omega_p + \mu_p)(\tau_p + \mu_p)}{\omega_p}\overline{I_p}],$$
$$\overline{E_p} = \frac{\tau_p + \mu_p}{\omega_p}\overline{I_p},$$
$$\overline{I_p} = \frac{\pi_p\omega_p}{(\omega_p + \mu_p)(\tau_p + \mu_p)} - \frac{\pi\pi_p\mu_p}{\eta_p\mu_p\pi + \eta_w N_h\alpha_h\pi_p},$$
$$\overline{R_p} = \frac{\tau_p}{\mu_p}\overline{I_p},$$
$$\overline{V_p} = \frac{N_h\alpha_h}{\pi}\overline{I_p}. \tag{4.2}$$

It can be seen from the definition of $\overline{I_p}$ that the endemic equilibrium $\overline{E}$ exists only when $\mathcal{R}_0 > 1$.

Theorem 2: The endemic equilibrium $\overline{E}$ of the system 3.1 is locally asymptotically stable if $\mathcal{R}_0 > 1$.

Proof: It can be seen from the above discussions that the endemic equilibrium $\overline{E}$ exists only when $\mathcal{R}_0 > 1$. And also from theorem 1 the DFE E^0 is unstable in such a case. Moreover, as the system 3.1 admits only two equilibria from the uniqueness and boundedness of solutions for the system 3.1 we conclude that the endemic equilibrium $\overline{E}$ is asymptotically stable whenever it exists *i.e.*, whenever $\mathcal{R}_0 > 1$.

5 Numerical simulations

The multi scale model 2.1 is uni-directionally coupled such that only the within-host scale sub model influences the between-host scale sub model without any reciprocal feedback. Owing to this, in this section, we study and numerically illustrate the influence of the four within-host scale sub model parameters, namely β, α, $d(= d_1 + \cdots + d_6)$ and $b(= b_1 + \cdots + b_6)$ on the between-host scale sub model variables (S_p, E_p, I_p, R_p, V_p).

Figure 1 depicts that as the infected cell burst rate increases, SARS-CoV-2 transmission in the community also increases. Therefore, drugs that inhibit viral replication (such as Arbidol, remdesivir, Lopinavir/Riton-
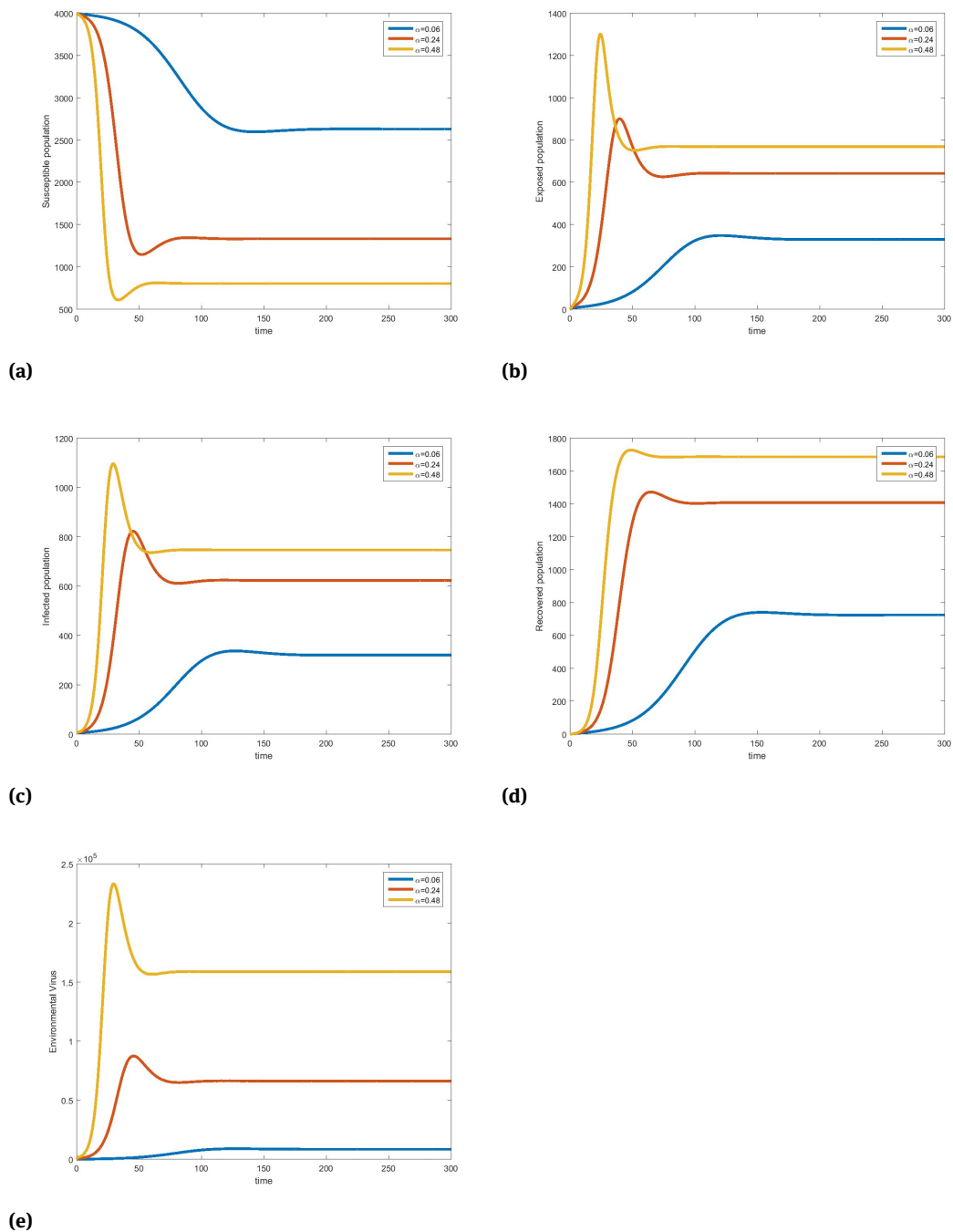
(a)

(b)

(c)

(d)

(e)

Figure 1: Effects of variation of production rate of virus from within-host infected cells (α).

avir) which in turn reduce the production rate of virus at within-host scale will likely reduce transmission of SARS-CoV-2 at between-host scale.

Figure 2 depicts that the antiviral drugs (such as Hydroxychloroquine (HCQ)) that reduce infection rate of susceptible epithelial cells may have individual level benefits but have insignificant population level benefits.

Figure 3 depicts that as the rate of clearance of free virus particles increases, SARS-CoV-2 transmission in the community also decreases. Therefore, treatments that increase the rate of clearance of free virus particles
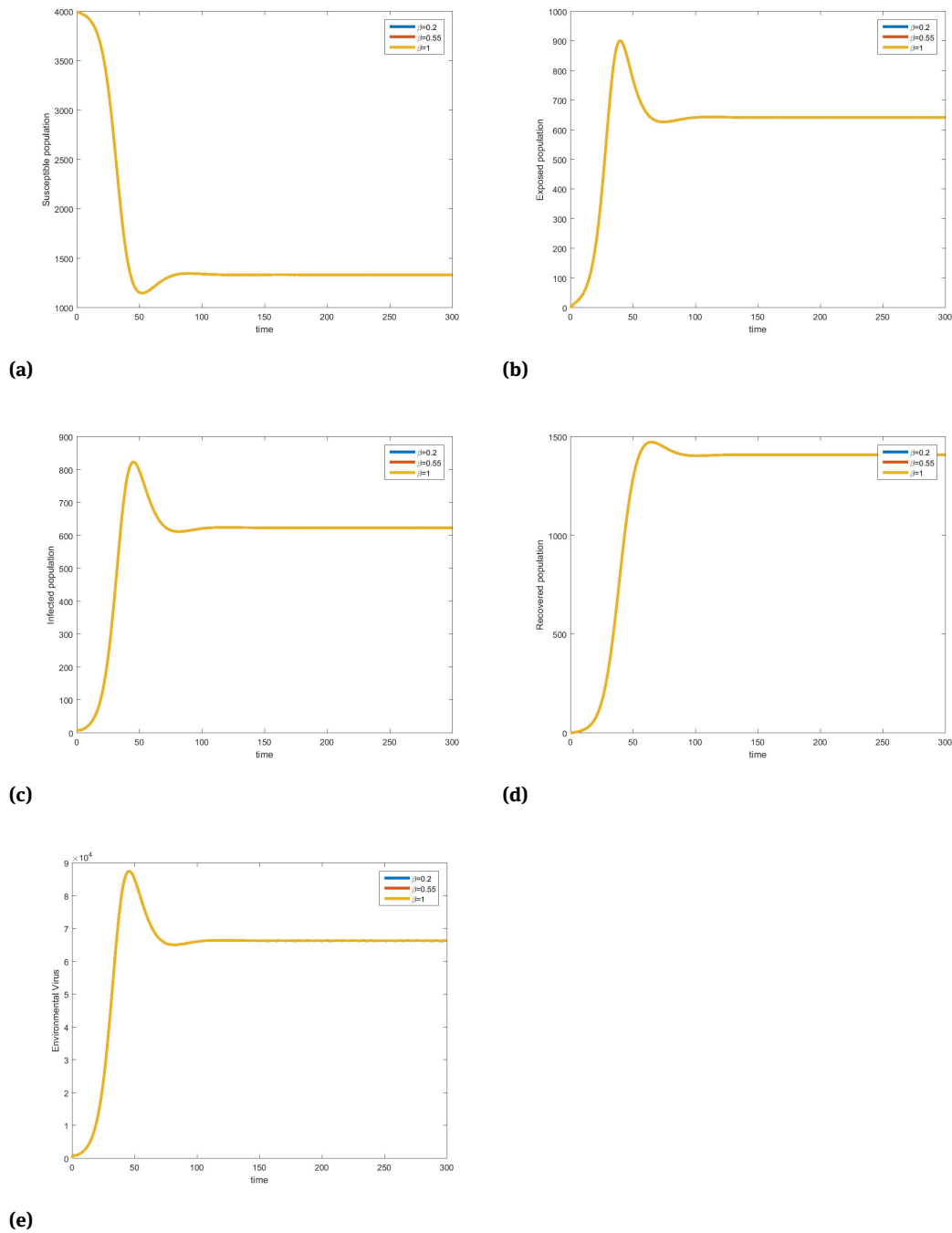
(a)

(b)

(c)

(d)

(e)

Figure 2: Effects of variation of infection transmission probability (β).

in an infected individual have potential community-level benefits of reducing SARS-CoV-2 transmission at between-host scale apart from benefits to the infected individual.

Figure 4 depicts that as the rate of killing of infected cells by immune system increases, SARS-CoV-2 transmission in the community also decreases slightly. Therefore, immunotherapies such as monoclonal antibodies that kill infected cells have potential community level benefits of reducing SARS-CoV-2 transmission at between-host scale apart from benefits to the infected individual.
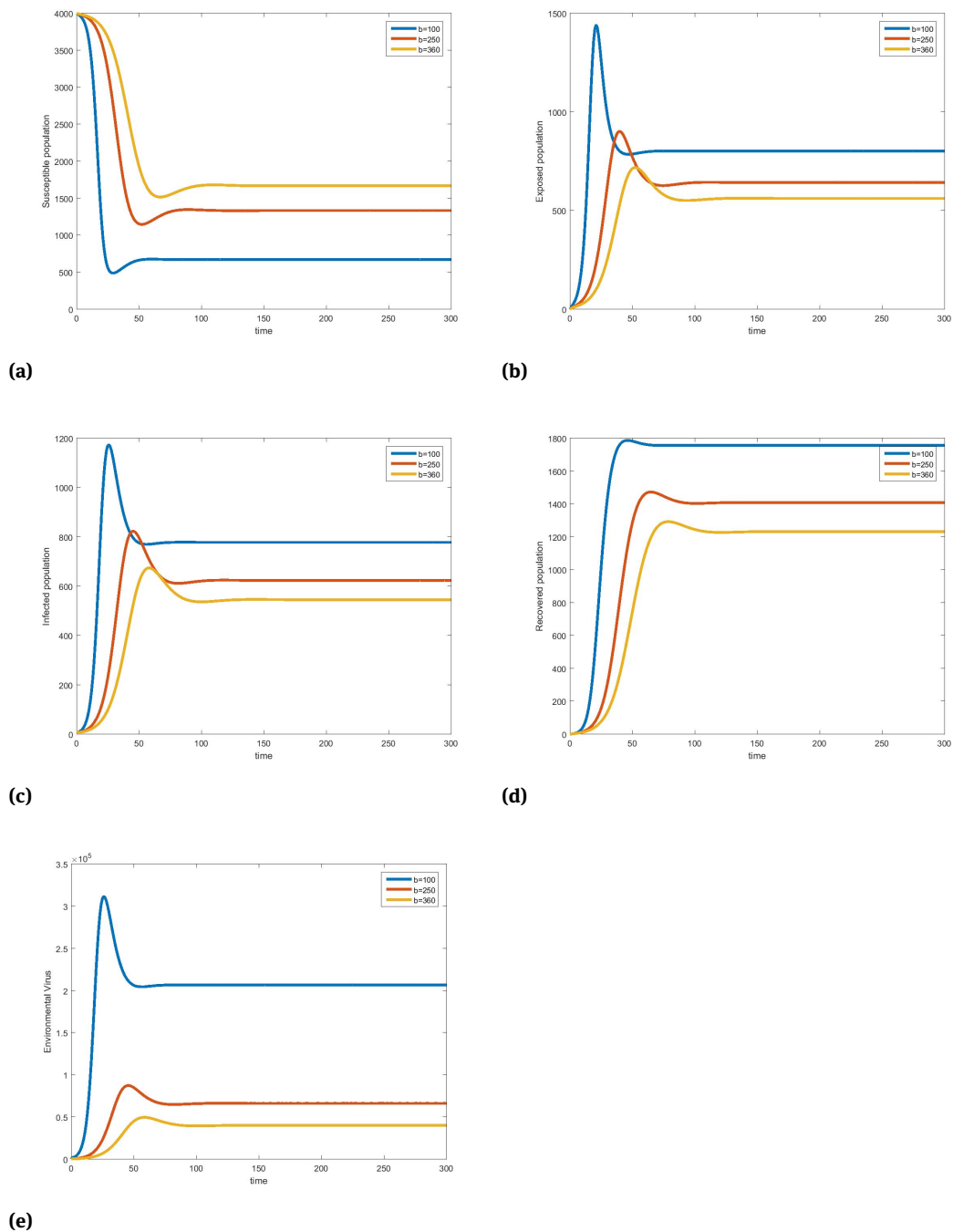
(a)

(b)

(c)

(d)

(e)

Figure 3: Effects of variation of clearance rate of virus by immune system (b).

6 Evaluating the comparative effectiveness of health interventions dealing with within-host and between-host scales

In this section we do the comparative effectiveness studies. We consider the following four health interventions dealing with within-host and between-host scales.
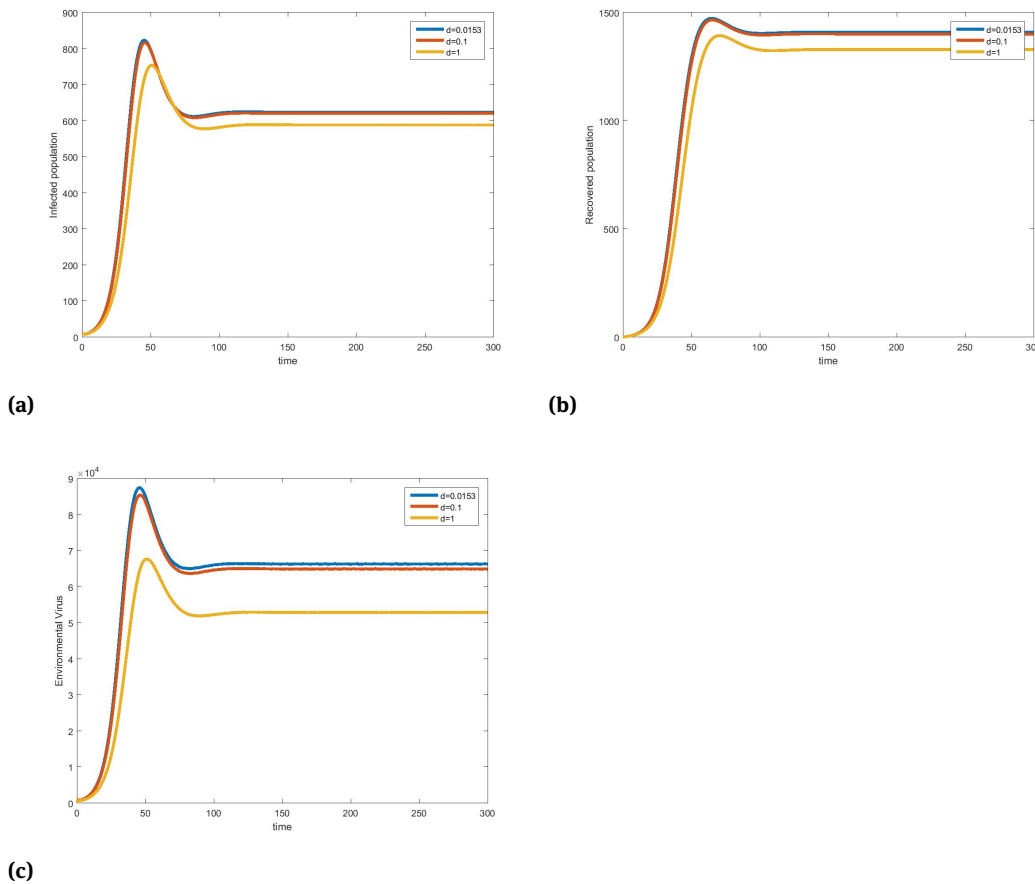
(a)

(b)

(c)

Figure 4: Effects of variation of rate of killing of infected cells by immune system (d).

1. Antiviral drugs:
   a. Drugs that inhibit viral replication: Drugs such as Arbidol, remdesivir, Lopinavir/Ritonavir inhibit viral replication in infected cells. So we choose α to be $\alpha(1 - \epsilon)$.
   b. Drugs that block virus binding to susceptible cells : Drugs such as Hydroxychloroquine (HCQ) does this job. So we choose β to be $\beta(1 - \gamma)$.
2. Immunotherapies : In this intervention the rate of clearance of virus increases due to antibodies. This in turn reduces the number of infected cells. So we choose $(d_1 + d_2 + d_3 + d_4 + d_5 + d_6)$ to be $(d_1 + d_2 + d_3 + d_4 + d_5 + d_6)(1 + \kappa)$.
3. Environmental hygiene: Decontamination from frequently touched spaces like door handles etc., reduces environmental virus. So we choose π to be $\pi(1 + \delta)$.
4. Generalized Social distancing: No mass gatherings, prayer meetings and educational institutions reduces contact with community viral load. So we choose η_w to be $\eta_w(1 - \sigma)$.

$\mathcal{R}_0$ plays a crucial role in understanding the spread of infection in the individual and $\overline{V_p}$ determines the infectivity of virus in an individual. Taking these four health interventions into consideration, we now have modified basic reproductive number $\mathcal{R}_E$ and modified virus count $\overline{V_E}$ of the endemic equilibrium to be

$$\mathcal{R}_E = \frac{1}{2(\omega_p + \mu_p)(\tau_p + \mu_p)}\left[\eta_p\omega_p(1 - \sigma) + \sqrt{(\eta_p\omega_p)^2(1 - \sigma)^2 + \frac{4\eta_w\pi_pN_e\alpha_h\omega_p}{\mu_p\pi(1 + \delta)}(\omega_p + \mu_p)(\tau_p + \mu_p)}\right]$$

$$\overline{V_E} = \frac{N_e\alpha_h\pi_p}{\omega_p}\left[\frac{\omega_p}{(\omega_p + \mu_p)(\tau_p + \mu_p)} - \frac{\pi(1 + \delta)\mu_p}{\eta_p\mu_p\pi(1 + \delta)(1 - \sigma) + \eta_wN_e\alpha_h\pi_p}\right]$$

where, N_e is the modified N_h given by,

$$N_e = \frac{\mathfrak{R}_e}{\beta(1-\gamma)}[1 - e^{-\mathfrak{R}_e} - \mathfrak{R}_e e^{-2\mathfrak{R}_e}],$$

$$\mathfrak{R}_e = \frac{\alpha\beta(1-\epsilon)(1-\gamma)S_h(s_{d_1})}{(b_1 + b_2 + b_3 + b_4 + b_5 + b_6 + \alpha_h)(\mu + (d_1 + d_2 + d_3 + d_4 + d_5 + d_6)(1+\kappa))}$$

We now do the comparative effectiveness study of these interventions by calculating the percentage reduction of $\mathcal{R}_0$ and $\overline{V_p}$ for single and multiple combination of these interventions at different efficacy levels such as (a) low efficacy of 0.3, (b) medium efficacy of 0.6, and (c)high efficacy of 0.9.

Percentage reduction of $\mathcal{R}_0$ and $\overline{V_p}$ are given by

Percentage reduction of $\mathcal{R}_0 = \left[\frac{\mathcal{R}_0 - \mathcal{R}_{E_j}}{\mathcal{R}_0}\right] \times 100,$

Percentage reduction of $\overline{V_p} = \left[\frac{\overline{V_p} - \overline{V}_{E_j}}{\overline{V_p}}\right] \times 100$

where j stands for ϵ, δ, κ, δ, σ or combinations thereof.

We now consider 20 different combinations of these four health interventions. Then for each efficacy level, we rank the percentage reductions on $\mathcal{R}_0$ and $\overline{V_p}$ in ascending order from 1 to 20 corresponding to the different combinations of five health interventions considered in this study. The comparative effectiveness is calculated and measured on a scale from 1 to 20 with 1 denoting the lowest comparative effectiveness while 20 denoting the highest comparative effectiveness. In Table 3 and 4, the abbreviations a) CEL stands for "Comparative Effectiveness at Low efficacy," which is 0.3, b) CEM stands for "Comparative Effectiveness at Medium efficacy," which is 0.6, c) CEH stands for "Comparative Effectiveness at High efficacy," which is 0.9.

Table 3: Comparative effectiveness for $\mathcal{R}_0$

No.	Indicator	%age	CEL	%age	CEM	%age	CEH
1	$\mathcal{R}_0$	0	1	0	1	0	1
2	$\mathcal{R}_{\mathcal{E}_\epsilon}$	16.34	12	36.75	12	68.38	12
3	$\mathcal{R}_{\mathcal{E}_\gamma}$	0	2	0	2	0	2
4	$\mathcal{R}_{\mathcal{E}_\kappa}$	1.79	4	3.47	4	5.09	4
5	$\mathcal{R}_{\mathcal{E}_\delta}$	12.29	5	20.94	5	27.45	5
6	$\mathcal{R}_{\mathcal{E}_\sigma}$	0.02	3	0.03	3	0.05	3
7	$\mathcal{R}_{\mathcal{E}_{\epsilon\delta\sigma}}$	26.62	15	50	15	77.06	15
8	$\mathcal{R}_{\mathcal{E}_{\gamma\delta\sigma}}$	12.29	7	20.94	7	27.45	7
9	$\mathcal{R}_{\mathcal{E}_{\kappa\delta\sigma}}$	13.86	10	23.69	10	31.14	10
10	$\mathcal{R}_{\mathcal{E}_{\epsilon\delta}}$	26.62	13	49.99	13	77.06	13
11	$\mathcal{R}_{\mathcal{E}_{\gamma\delta}}$	12.29	6	20.94	6	27.45	6
12	$\mathcal{R}_{\mathcal{E}_{\kappa\delta}}$	13.86	8	23.69	8	31.14	8
13	$\mathcal{R}_{\mathcal{E}_{\epsilon\gamma\delta}}$	26.62	14	49.99	14	77.06	14
14	$\mathcal{R}_{\mathcal{E}_{\epsilon\kappa\delta}}$	27.93	18	51.74	18	78.23	18
15	$\mathcal{R}_{\mathcal{E}_{\gamma\kappa\delta}}$	13.86	9	23.69	9	31.14	9
16	$\mathcal{R}_{\mathcal{E}_{\epsilon\gamma\kappa\delta}}$	27.93	17	51.74	17	78.23	17
17	$\mathcal{R}_{\mathcal{E}_{\epsilon\gamma\delta\sigma}}$	26.62	16	50	16	77.06	16
18	$\mathcal{R}_{\mathcal{E}_{\epsilon\kappa\delta\sigma}}$	27.93	20	51.74	20	78.23	20
19	$\mathcal{R}_{\mathcal{E}_{\gamma\kappa\delta\sigma}}$	13.86	11	23.69	11	31.14	11
20	$\mathcal{R}_{\mathcal{E}_{\epsilon\gamma\kappa\delta\sigma}}$	27.93	19	51.74	19	78.23	19

The outcomes of the comparative effectiveness study suggest the following.

Table 4: Comparative effectiveness for $\overline{V_p}$

No.	Indicator	%age	CEL	%age	CEM	%age	CEH
1	$\overline{V_p}$	0	1	0	1	0	1
2	$\overline{V_{E_\epsilon}}$	30.00	12	60.00	12	90.00	12
3	$\overline{V_{E_\gamma}}$	0	2	0	2	0	2
4	$\overline{V_{E_\kappa}}$	3.54	7	6.84	7	9.92	7
5	$\overline{V_{E_\delta}}$	0.01	5	0.01	5	0.01	5
6	$\overline{V_{E_\sigma}}$	0.01	3	0.01	3	0.01	3
7	$\overline{V_{E_{\epsilon\delta\sigma}}}$	30.00	15	60.00	15	90.00	15
8	$\overline{V_{E_{\gamma\delta\sigma}}}$	0.01	6	0.01	6	0.01	6
9	$\overline{V_{E_{\kappa\delta\sigma}}}$	3.54	11	6.84	11	9.92	11
10	$\overline{V_{E_{\epsilon\delta}}}$	30.00	13	60.00	13	90.00	13
11	$\overline{V_{E_{\gamma\delta}}}$	0.01	4	0.01	4	0.01	4
12	$\overline{V_{E_{\kappa\delta}}}$	3.54	9	6.84	9	9.92	9
13	$\overline{V_{E_{\epsilon\gamma\delta}}}$	30.00	14	60.00	14	90.00	14
14	$\overline{V_{E_{\epsilon\kappa\delta}}}$	32.48	18	62.74	18	91,00	18
15	$\overline{V_{E_{\gamma\kappa\delta}}}$	3.54	8	6.84	8	9.92	8
16	$\overline{V_{E_{\epsilon\gamma\kappa\delta}}}$	32.48	17	62.74	17	90.99	17
17	$\overline{V_{E_{\epsilon\gamma\delta\sigma}}}$	30.00	16	60.00	16	90.00	16
18	$\overline{V_{E_{\epsilon\kappa\delta\sigma}}}$	32.48	20	62.74	20	90.99	20
19	$\overline{V_{E_{\gamma\kappa\delta\sigma}}}$	3.54	10	6.84	10	9.92	10
20	$\overline{V_{E_{\epsilon\gamma\kappa\delta\sigma}}}$	32.48	19	62.74	19	90.99	19

1. When a single strategy is implemented, treatment with drugs such as Arbidol, remdesivir, Lopinavir/Ritonavir that inhibits viral replication show significant decrease of $\mathcal{R}_0$ relative to other four interventions at all efficacy levels. We deduced this with reference to the entries 2-6 in Table 3 and Table 4.
2. Considering the severity of this pandemic, one single strategy is not sufficient to tackle this infection at the earliest. When environmental hygiene and generalized social distancing are implemented along with treatment of single drug, treating with drugs that inhibits viral replication performs better again at all efficacy levels. We deduced this with reference to the entries 7-9 in Table 3 and Table 4.
3. Now that governments are accepting the fact that we have to live with the virus for long and planning for unlock strategies, generalized social distancing like closure of schools does not seem practical. By considering only environmental hygiene, along with the drugs that inhibits viral replication seem to perform twice better than other drugs at all efficacy levels. We deduced this with reference to the entries 10-19 in Table 3 and Table 4.
4. A combined strategy involving treatment with drugs such as Arbidol, remdesivir, Lopinavir/Ritonavir that inhibits viral replication and immunotherapies like monoclonal antibodies, along with environmental hygiene and generalized social distancing seems to perform the best among all combinations considered at all efficacy levels. We deduced this with reference to the entry 20 in Table 3 and Table 4.

7 Discussion and Conclusions

In this work a novel nested multi scale model for COVID-19 is proposed and studied. We initially study the dynamics of this system and do the stability analysis. Later using the technique of comparative effectiveness we study the efficacy of four health interventions dealing with within-host and between-host scales. The results suggest that a combined strategy involving treatment with drugs such as Arbidol, remdesivir, Lopinavir/Ri-

tonavir that inhibits viral replication and immunotherapies like monoclonal antibodies, along with environmental hygiene and generalized social distancing proved to be the best and optimal in reducing the basic reproduction number and environmental virus at the population level.

With a lot of research happening in the field of multi-drug therapy, our results offer some basic insights of their efficiency and effectiveness at population scale. These results can be helpful in public health measures and policies. With more availability of data of within-host dynamics in COVID-19 patients, a better refined and comprehensive models can be framed based on this that can be more closer to real life situations. The multi scale modeling studies done here is the first of its kind for COVID-19.

References

[1] *https://www.worldometers.info/coronavirus/*.

[2] Praveen Agarwal and Ram Singh, *Modelling of transmission dynamics of nipah virus (niv): a fractional order approach*, Physica A: Statistical Mechanics and its Applications (2020), 124243.

[3] Kaustuv Chatterjee, Kaushik Chatterjee, Arun Kumar, and Subramanian Shankar, *Healthcare impact of covid-19 epidemic in india: A stochastic mathematical model*, Medical Journal Armed Forces India (2020).

[4] Edmund X DeJesus and Charles Kaufman, *Routh-hurwitz criterion in the examination of eigenvalues of a system of nonlinear ordinary differential equations*, Physical Review A **35** (1987), no. 12, 5288.

[5] Jeffrey W Eaton, Leigh F Johnson, Joshua A Salomon, Till Bärnighausen, Eran Bendavid, Anna Bershteyn, David E Bloom, Valentina Cambiano, Christophe Fraser, Jan AC Hontelez, et al., *Hiv treatment as prevention: systematic comparison of mathematical models of the potential impact of antiretroviral therapy on hiv incidence in south africa*, PLoS Med **9** (2012), no. 7, e1001245.

[6] Winston Garira and Dephney Mathebula, *Development and application of multiscale models of acute viral infections in intervention research*, Mathematical Methods in the Applied Sciences **43** (2020), no. 6, 3280–3306.

[7] Giulia Giordano, Franco Blanchini, Raffaele Bruno, Patrizio Colaneri, Alessandro Di Filippo, Angela Di Matteo, and Marta Colaneri, *Modelling the covid-19 epidemic and implementation of population-wide interventions in italy*, Nature Medicine (2020), 1–6.

[8] Muhammad Altaf Khan and Abdon Atangana, *Modeling the dynamics of novel coronavirus (2019-ncov) with fractional derivative*, Alexandria Engineering Journal (2020).

[9] Adam J Kucharski, Timothy W Russell, Charlie Diamond, Yang Liu, John Edmunds, Sebastian Funk, Rosalind M Eggo, Fiona Sun, Mark Jit, James D Munday, et al., *Early dynamics of transmission and control of covid-19: a mathematical modelling study*, The lancet infectious diseases (2020).

[10] Chentong Li, Jinhu Xu, Jiawei Liu, and Yicang Zhou, *The within-host viral kinetics of sars-cov-2*, bioRxiv (2020).

[11] Piu Samui, Jayanta Mondal, and Subhas Khajanchi, *A mathematical model for covid-19 transmission dynamics with a case study of india*, Chaos, Solitons & Fractals **140** (2020), 110173.

[12] Ram Singh, Naveen Sharma, and Aditi Ghosh, *Modeling assumptions, mathematical analysis and mitigation through intervention*, Letters in Biomathematics **6** (2019), no. 2, 1–19.

[13] Daniel A. Solomon, Amy C. Sherman, and Sanjat Kanjilal, *Influenza in the COVID-19 Era*, JAMA **324** (2020), no. 13, 1342–1343.

[14] Pauline Van den Driessche and James Watmough, *Reproduction numbers and sub-threshold endemic equilibria for compartmental models of disease transmission*, Mathematical biosciences **180** (2002), no. 1-2, 29–48.

[15] Esteban Abelardo Hernandez Vargas and Jorge X Velasco-Hernandez, *In-host modelling of covid-19 kinetics in humans*, medRxiv (2020).

[16] Carolin Vegvari, Christoforos Hadjichrysanthou, Emilie Cauet, Emma Lawrence, Anne Cori, Frank De Wolf, and Roy M Anderson, *How can viral dynamics models inform endpoint measures in clinical trials of therapies for acute viral infections?*, PloS one **11** (2016), no. 7.

[17] Huan-Xiang Zhou, *Theoretical frameworks for multiscale modeling and simulation*, Current opinion in structural biology **25** (2014), 67–76.